Phase-Only Matched Filtering of Ultrawideband Arbitrary Microwave Waveforms via Optical Pulse Shaping

Ehsan Hamidi, *Student Member, IEEE*, and Andrew M. Weiner, *Fellow, IEEE, Fellow, OSA*

(Invited Paper)

***Abstract*—We demonstrate compression of ultrawideband (UWB) microwave arbitrary waveforms via phase-only matched filtering implemented in a programmable hyperfine resolution optical pulse shaper. We synthesize spread-time UWB electrical waveforms and utilize programmable microwave photonic phase filters to impose the opposite of a waveform's spectral phase on its spectrum. This enables us to compress an UWB microwave waveform to its corresponding bandwidth-limited pulse duration via phase filtering. As an example, we present compression of a linear frequency-modulated electrical waveform with >15 GHz frequency content with almost 200% fractional bandwidth with ~ 733 ps temporal window to a 40-ps duration pulse with more than 14-dB gain in peak power. Our technique is programmable and we believe it is applicable to a wide range of arbitrary spectral phase modulated UWB radio frequency (RF) waveforms.**

***Index Terms*—Matched filters, microwave photonics, phase filters, pulse compression, optical pulse shaping, ultrawideband (UWB) systems.**

I. Introduction

THE FIELD of microwave photonics where optical techniques are utilized to enhance radio frequency (RF) systems performance has been developed significantly in the past few decades [1]–[13]. This covers a wide range of techniques: microwave photonic delay lines [1], [2], microwave photonic filters [3]–[8], and microwave photonic waveform generators [9]–[13], etc. The use of optical pulse shaping techniques followed by optical-to-electrical (O/E) conversion for the generation of arbitrary RF electrical waveforms with bandwidths exceeding the few GHz values available via commercial electronic arbitrary waveform technology has been recently demonstrated [9]–[11]. Although a lot of effort has been devoted to the generation of microwave waveforms via photonic techniques, still practical techniques for processing and detection of ultrawideband (UWB) electrical signals for applications in communication systems are lacking.

Manuscript received January 29, 2008; revised May 21, 2008. Current version published October 10, 2008. This work was supported in part by the National Science Foundation by Grant ECCS-0701448.

The authors are with the School of Electrical and Computer Engineering, Purdue University, West Lafayette, IN 47907 USA (e-mail: ehamidi@purdue.edu; amw@purdue.edu).

Digital Object Identifier 10.1109/JLT.2008.927175

One technique which is often utilized in communication systems to detect a specified signal pattern is the matched filter, which is often implemented via correlation. This technique is commonly used in direct sequence spread spectrum system receivers. In this technique, a received signal is multiplied with a proper despreading signal and integrated over time, and data is extracted from the resultant output signal [14], [15]. However, this technique requires synchronization of the reference despreading signal with the received signal and suffers from timing jitter [16], [17]. Another paper from our group, also submitted to this Special Issue, demonstrates matched filtering via correlation with a synchronized despreading waveform over UWB bandwidth [18].

Matched filter-based detection techniques can also be implemented using a time-invariant filter such that its time domain impulse response is a time-reversed version of the specified signal pattern. This operates similar to matched filters based on correlation; however, it has an advantage that it is real-time and does not require generation and synchronization of a specified despreading signal at the receiver, which significantly reduces complexity [14]. In microwave filter design area, the design of microwave arbitrary phase filters is untouched particularly for UWB applications; hence matched filters are generally implemented based on correlation instead of time-invariant filters. In principle, the time-invariant filter implementation of a matched filter for a waveform with uniform spectrum operates as a waveform compressor by compensation of the spectral phase. This concept of a matched filter acting as a pulse compressor has been extensively used in radar [19]. Although a matched filter also improves the signal-to-noise-ratio (SNR) for signals in additive Gaussian noise, here we only concentrate on the waveform compression aspect of a matched filter. In this paper, we use the terms matched filter and waveform compressor interchangeably.

A similar concept to the matched filter is utilized in spectrally encoded communication systems. The concept of spectral coding has been proposed both in an optical communication system in [20] and for a wireless communication system [21]. In this technique, a message signal is multiplied by a spreading code in the frequency domain, as opposed to conventional direct sequence code division multiple access systems in which the encoding is in the time domain. As a result, the signal will be spread in time. At the receiver, the received signal spectrum is multiplied by the conjugate of the spreading signal spectrum.

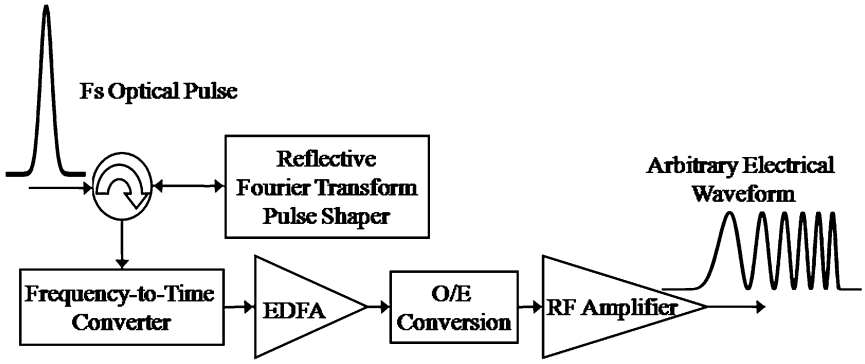

Fig. 1. Microwave photonic arbitrary waveform generator.

Hence this technique requires Fourier transform of signals since multiplication takes place in the frequency domain [21], [22]. In optical communication systems, spectral coding has been realized through Fourier transform pulse shaping [20], [23]. However in wireless communication systems, Fourier transform of signals is performed by an established implementation that corresponds to the multiplication and convolution of the desired signal by linear frequency-modulated waveforms using surface acoustic wave (SAW) devices [21]. Due to difficulties and challenges in fabricating SAW correlators, they have been demonstrated only for center frequencies up to 3.63 GHz with 1.1 GHz bandwidth (only 30% fractional bandwidth) with insertion loss of 23 dB even after accounting for the pulse compression gain [24]. This frequency bandwidth is well below the UWB frequency band (3.1–10.6 GHz) allocated by the Federal Communications Commission [25] and bandwidths accessible via RF photonic waveform generation techniques with almost 200% fractional bandwidth [9]–[11]. On the other hand, UWB receivers based on a digital signal processing scheme are limited by analog-to-digital converters' speed and dynamic range [16], [26]. State-of-the-art in implementing an electronic UWB receiver is also limited to bandwidths much less than the UWB frequency band [27]. Hence, photonic processing of microwave waveforms is an interesting candidate for processing UWB electrical signals in wireless systems [6].

In photonic processing of microwave signals, the RF waveform is generally modulated on an optical carrier and the optical signal is processed in the optical domain and then converted back into the RF domain through O/E conversion [3]. In the conventional technique, a photonic signal processing device is implemented through multitap optical delay lines. This scheme enables to design discrete-time microwave photonic filters with a finite impulse response that have been demonstrated as amplitude filters [4], [5]. However, little consideration has been given to spectral phase filters with an exception of true-time delay lines which correspond to a controllable linear spectral phase for beam forming in phased-array antennas [2].

Recently, programmable photonic microwave filters with arbitrary UWB phase/amplitude response were implemented via hyperfine resolution optical pulse shaping in a work by Xiao *et al.* [7], [8]. This unveils a new approach for detection of spread-time electrical waveforms, in general, and spectrally encoded electrical waveforms, in particular, in UWB wireless communication systems via matched filtering. Here we present, for the first time to the best of our knowledge, the application of this novel technique to realize programmable pulse compression of UWB RF electrical waveforms with almost 200% fractional bandwidth through time-invariant matched filtering.

This paper is organized as follows. In Section II, we will discuss our experimental setup and the basics of microwave arbitrary waveform generation via optical pulse shaping and microwave photonic filtering based on hyperfine resolution optical pulse shaping, which form waveform generator and compressor subsystems in our technique respectively. A theoretical analysis is discussed in Section III. Experimental and numerical results on matched filtering will be presented in Section IV, and in Section V, we will conclude.

II. Experimental Setup

Our experimental setup consists of two separate subsystems: a microwave photonic filter which is programmed to function as a matched filter and a microwave photonic arbitrary waveform generator which is used to test the matched filter operation. In the following, we first discuss the waveform generator and then the microwave photonic programmable filter.

A. Microwave Photonic Arbitrary Waveform Generator

A schematic of our microwave arbitrary waveform generator based on the method of [11] is shown in Fig. 1. In the arbitrary waveform generator, we utilize a technique for synthesis of arbitrary microwave waveforms based on ultrafast optical arbitrary waveform technology [9], [10]. As shown in Fig. 1, this apparatus consists of a mode-locked fs fiber laser, a Fourier transform optical pulse shaper [23], an optical frequency-to-time converter, an erbium-doped fiber amplifier (EDFA), an O/E converter, and an RF amplifier. A detailed description of this apparatus is given in [10] and [11].

Ultrashort optical pulses from the mode-locked laser ($\sim$100 fs, 50 MHz repetition rate) are spectrally filtered in the reflective-geometry Fourier transform optical pulse shaper which enables to impose a user-defined optical filter function onto the power spectrum of the optical pulses. The output pulses are dispersed in 1.6 km of single-mode optical fiber which uniquely maps optical frequency to time and results in a temporal inten-

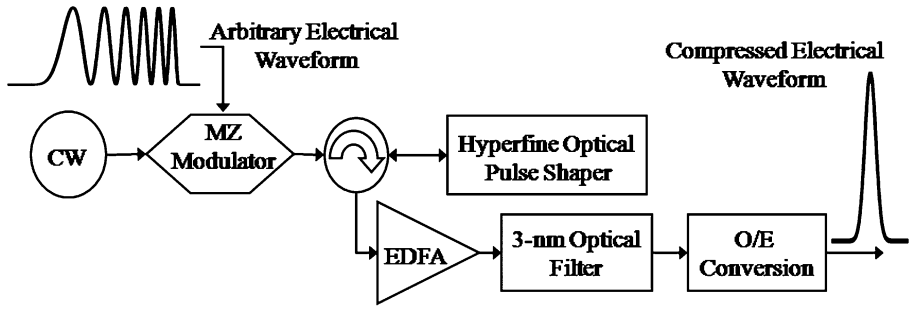

Fig. 2. Microwave photonic programmable matched filter.

sity profile which is a scaled version of the filter function applied in the optical pulse shaper.

The output tailored optical intensity waveforms are converted to electrical signals via O/E conversion in a photodiode with an electrical 3-dB bandwidth of $\sim$22 GHz. The RF electrical output of the photodiode is amplified with a broadband microwave amplifier (0.1–18 GHz, $\sim$29 dB gain) to be applied to an optical intensity modulator in the next stage. Currently we can achieve 0.7 V peak-to-peak electrical waveforms.

The time aperture of the generated waveforms is determined by the optical bandwidth and the length of the fiber stretcher [10]. In our setup the length of the fiber stretcher has been chosen 1.6 km in order to obtain waveforms with about 750 ps temporal window which is the time aperture of the microwave photonic filter setup.

B. Microwave Photonic Programmable Matched Filter

A schematic of a microwave photonic programmable waveform compressor/matched filter is shown in Fig. 2. Our microwave photonic programmable matched filter is based on programmable microwave photonic filters demonstrated in [7], [8]. This technique uses optical frequency domain filtering with O/E conversion, rather than the traditional tapped delay line approach. The frequency domain optical filtering is based on Fourier transform pulse shaping [23], which has been extended to hyperfine ($\sim$600 MHz) spectral resolution [8] through the use of a virtually imaged phased array (VIPA) as a spectral disperser [28]. In this technique, the phase/amplitude filter imposed onto the optical spectrum is directly mapped onto a microwave phase/amplitude filter at the output. As a result, a user-defined frequency domain microwave phase/amplitude filter is implemented photonically that provides programmable and essentially arbitrary phase/amplitude filter response over RF band from dc to 20 GHz with $\sim$600 MHz spectral resolution [7], [8].

The minimum spectral resolution of a pulse shaper determines the maximum temporal window of a waveform, which can be manipulated, where their relation is given by the time-bandwidth product [23]. A spectral resolution of $\sim$600 MHz corresponds to a temporal window of about 730 ps. In order to match the generated microwave waveforms' temporal aperture to the microwave photonic filter spectral resolution, we have adjusted the temporal window of waveforms generated in the microwave photonic arbitrary waveform generator to about 750 ps.

In this setup, a tunable laser with linewidth below 0.1 pm centered at 1550.17 nm is input to a Mach-Zehnder (MZ) intensity modulator with an electrical 3-dB bandwidth of 30 GHz and a minimum transmission voltage of $V_\pi \sim 4.75$ V, which is driven with a microwave arbitrary waveform generated via the microwave photonic arbitrary waveform generator explained formerly. Proper operation of our waveform compressor requires that the optical carrier linewidth and frequency drift should be much less than the minimum spectral resolution of the optical pulse shaper, which is satisfied by our continuous wavelength (CW) laser with 0.1 pm (12.5 MHz) linewidth. In our experiment, the MZ modulator (MZM) is biased very close to its minimum transmission. As a result, the output optical intensity is negligible when the electrical input is zero, and for positive values of ac voltage input the optical carrier electric field is modulated with electrical waveform so that the RF waveform maps directly to the envelope of the optical carrier electric field [29]. Modulating the optical carrier with a UWB RF electrical waveform in the MZM transfers the RF signal into the optical domain as a double-sideband modulation about the optical carrier. The resulting double-sideband modulated signal is applied to an optical pulse shaper. In our experiment, we allow both sidebands to pass through the optical pulse shaper, as opposed to [8] where one sideband is suppressed.

Fig. 3 illustrates a hyperfine resolution optical pulse shaper configuration. As in Fourier transform pulse shaping [23], different optical frequency components contained within the input signal are first separated spatially using an optical spectral disperser and a lens, and then a spatial light modulator (SLM) manipulates the phase/amplitude of the different frequency components in parallel. By using a polarizer at the pulse shaper input, simultaneous and independent amplitude and phase filtering of individual optical frequency components are enabled [7], [8], [23]. A detailed description of such hyperfine resolution pulse shapers used for programmable microwave photonic filtering is given in [7] and [8].

The output of the hyperfine optical pulse shaper is applied to an EDFA. After amplification in an EDFA, the optical signal passes through a 3-nm optical filter to reduce its amplified spontaneous emission. Then the spectrally-filtered optical signal is converted to a baseband electrical signal via a photodiode with an electrical 3-dB bandwidth of $\sim$22 GHz. The resultant microwave signal is measured by a fast sampling scope.

The Fourier transform pulse shaper acts as a bandpass filter on the modulated optical signal. By programming the SLM,

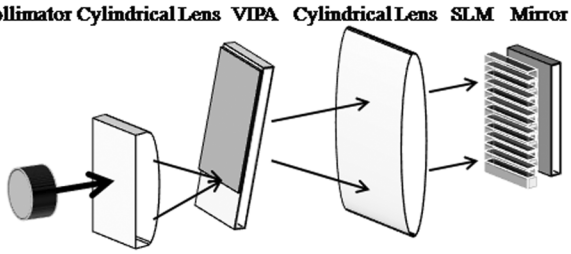

Fig. 3. Hyperfine resolution optical pulse shaper: virtually imaged phased array (VIPA); spatial light modulator (SLM).

a filter with an arbitrary spectral phase/amplitude can be synthesized and imposed on the optical signal. For practical signals which are real, one sideband is a complex-conjugate of the other; thus in our apparatus, an optical filter is implemented with complex-conjugate symmetry about the optical carrier frequency. In order to program the microwave photonic filter as a matched filter, we first extract the spectrum of the output uncompressed electrical waveform when the pulse shaper is quiescent, i.e., no spectral phase is added, by taking Fourier transform of the measured output waveform. By imposing the conjugate of the output uncompressed waveform's spectrum, which reduces to only spectral phase for uniform broadband RF signals, on its corresponding optical signal spectrum the envelope of the optical carrier electric field is compressed to its transform-limited duration via matched filtering that results in corresponding output compressed transform-limited duration electrical pulse through O/E conversion.

III. Theoretical Discussion

For a signal s(t), a filter which is matched to s(t) has an impulse response, in general, given by $h(t) = k\,s(t_0 - t)$ where k and t_0 are arbitrary constants. It can be shown that the SNR of a received signal plus additive white Gaussian noise can be maximized by the operation of a linear filter which is matched to the signal s(t) on a received signal. More detail on the theory of matched filters is given in [14] and [15].

A matched filter may be designed in frequency domain instead of time domain as a spectral filter where its frequency response relates to its impulse response through Fourier transform. Without loss of generality, we investigate waveforms which almost uniformly cover the UWB bandwidth and beyond. Since a signal with almost uniform spectrum content corresponds to a matched filter with almost uniform spectral amplitude, we can approximate its matched filter as a spectral phase-only filter. Therefore, the resulting matched filter has a spectral phase which is the opposite of a specified signal spectral phase as $H(\omega) = e^{-j\angle S(\omega)}$. This results in compression of spectral phase-modulated input signals to the bandwidth limit. This pulse compression aspect of matched filters is the focus of our investigation.

In general a matched filter is usually designed to operate as a baseband filter. However, the possibility of implementing a matched filter in the optical domain via microwave photonic filters enables us to achieve a broadband matched filter. Fig. 4 shows a simplified block diagram of a microwave photonic

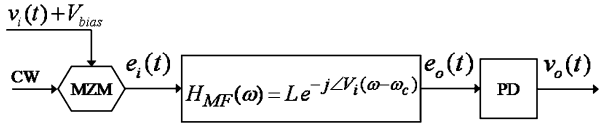

Fig. 4. Simplified microwave photonic phase-only matched filter block diagram.

matched filter where the distortion due to the MZM, the frequency response roll-off of the modulator, the photodiode (PD) and the pulse shaper, and the nonlinearity of the EDFA, which is a slow saturable optical amplifier, are neglected. The MZM output light electric field e as a function of the driving voltage V is given by $e = e_0 \cos[(\pi V/V_\pi + \phi)/2]$ where e_0 is the input light electric field, V_π is the half-wave voltage, and ϕ is a static phase shift [29]. Assuming small signal operation such that the MZM is biased about $\mathrm{V} = \mathrm{V}_\pi$ and for simplicity $\phi = 0$ through first-order approximation we have $e \approx -e_0[\pi(V - V_\pi)/2V_\pi]$ where $\mathrm{v_i} = \mathrm{V} - \mathrm{V_{bias}}$ is a small signal input voltage. An input electrical voltage signal $\mathrm{v_i}(\mathrm{t})$ with a one-sided bandwidth of B is applied with an appropriate bias voltage $\mathrm{V_{bias}}$ to the MZM. Modulating the electric field of an optical carrier results in an optical electric field $\mathrm{e_i}(\mathrm{t})$ which is input to an optical pulse shaper as

$$e_i(t) = \alpha[\, v_i(t) + V_{\mathrm{bias}} - V_\pi]\, e_0 \cos(\omega_c t) \tag{1}$$

where $\alpha = -\pi/2\mathrm{V}_\pi$ is the linear term of the modulation coefficient determined by the slope of a tangent to the modulator transmission curve at the operating point, $\mathrm{e_0}$ is the input optical carrier electric field amplitude, and ω_c is the optical carrier angular frequency. The resulting passband optical signal passes through an optical filter that when the pulse shaper is programmed with the conjugate of the electrical waveform spectral phase, its frequency response is

$$H_{\mathrm{MF}}(\omega) = L\left[e^{-j\angle V_i(\omega-\omega_c)} + e^{+j\angle V_i(-\omega-\omega_c)}\right] \tag{2}$$

where L accounts for the optical pulse shaper spectral loss, which in general, is a function of angular frequency ω and in our pulse shaper it rolls off $\sim$3 dB over a 20–GHz bandwidth. However, we approximate it as a constant. Further details on microwave photonic filter spectral response is given in [8]. In (2), the first and second terms in brackets represent the matched filter in positive and negative frequencies respectively; however, in Fig. 4, we only show the frequency response for positive frequencies. We can find the output optical electric field after passing through the matched filter through Fourier transform as

$$\begin{aligned} e_o(t) &= F^{-1}\{H_{\mathrm{MF}}(\omega)E_i(\omega)\} \\ &= L\alpha e_0 \left\{F^{-1}\{|V_i(\omega)|\} + V_{\mathrm{bias}} - V_\pi\right\}\cos(\omega_c t) \end{aligned} \tag{3}$$

and when there is no spectral phase is added, the output electric field spectrum after passing through the pulse shaper is simply $e_o(t) = L\, e_i(t) = L\alpha[v_i(t) + V_{\mathrm{bias}} - V_\pi]\, e_0 \cos(\omega_c t)$.

A photodiode maps its input optical intensity to an electrical signal and it operates as a square-law detector where its output electrical voltage signal is proportional to the square of its input optical electric field $v_o(t) = \kappa\langle e_o^2(t)\rangle$ where κ is the (O/E)

conversion coefficient. Thus from (3) we find the photodiode output compressed electrical signal when the matched filter is applied as:

$$v_o(t) = \frac{1}{2}\kappa L^2\alpha^2 e_0^2 \left[F^{-1}\{|V_i(\omega)|\} + V_{\rm bias} - V_\pi\right]^2 \quad (4)$$

The output uncompressed electrical signal, when the pulse shaper adds no spectral phase, becomes:

$$v_o(t) = \frac{1}{2}\kappa L^2\alpha^2 e_0^2 \left[v_i(t) + V_{\rm bias} - V_\pi\right]^2 \quad (5)$$

Here we give two definitions to compare the output uncompressed and compressed voltage waveforms in order to evaluate a waveform compressor performance. We define a gain parameter as the ratio of the compressed pulse peak voltage, minus its dc level, to the uncompressed waveform peak voltage, minus its dc level, all measured after the photodiode, as $\gamma = (V_c - {\rm dc}_c)/(V_u - {\rm dc}_u)$, where subscripts "c" and "u" denote "compressed" and "uncompressed" respectively. γ can be expressed in decibels (dB) as $\gamma({\rm dB}) = 20\log(\gamma)$. Since a photodiode maps optical intensity to an electrical signal, the resulting voltage signal is required to be a positive-definite quantity and has a non-zero dc level. The subtraction of the dc voltage is relevant since a dc voltage carries no information and may be easily blocked by a dc blocker. We also define a compression factor as the ratio of the uncompressed voltage waveform temporal window $\Delta{\rm T}$ to the compressed voltage pulse full width at half maximum (FWHM) duration $\Delta{\rm t}$, all measured after subtraction of their dc levels, as $\eta = \Delta T/\Delta t$. Note that the pulse FWHM duration is most meaningful for a waveform with no dc level, and it gives a measure of frequency bandwidth for signals with no dc level. Therefore the temporal pulse width has been measured after subtraction of the dc level, which has information about frequency content of the pulse.

Following we briefly provide a simple analysis which describes the relation between a gain parameter, a compression factor, and a bandwidth to characterize the performance of a waveform compressor. We consider an electrical voltage signal ${\rm v_i(t)}$ with a spectrum uniformly equal to ${\rm S_0}$ from -B to B in the baseband and zero elsewhere. The electrical signal spectral phase is assumed arbitrary, however we are interested in a spectral phase which spreads the signal ${\rm v_i(t)}$ quite uniformly over its time aperture $\Delta{\rm T}$. By appropriately designing this spread-time waveform, the energy of the waveform may be evenly spread over its time window. However an arbitrary electrical waveform generated via the microwave photonic waveform generator is a definite-positive voltage signal, since the photodiode has a definite positive output voltage. Hence, we assume the signal ${\rm v_i(t)}$ takes definite positive values over its temporal window and zero elsewhere. As a result the uncompressed electrical signal ${\rm v_i(t)}$ contains a positive dc voltage over its time aperture which is

$${\rm dc}_v = \frac{1}{\Delta T}\int_0^{\Delta T} v_i(\tau)d\tau. \quad (6)$$

We also assume that the signal ${\rm v_i(t)}$ has a constant ac energy equal to U where we can show through Parseval's equation that $S_0 = \sqrt{U/2B}$.

From foregoing assumptions we approximate

$$F^{-1}\{|V_i(\omega)|\} \cong \begin{cases} S_0\frac{\sin(2\pi B\,t)}{\pi\,t} + {\rm dc}_v & \text{for } -\Delta{\rm T}/2 \le {\rm t} \le \Delta{\rm T}/2 \\ 0 & \text{elsewhere.} \end{cases} \quad (7)$$

Equation (7) is an approximation which roughly holds over the time aperture of the signal from $-\Delta{\rm T}/2$ to $\Delta{\rm T}/2$. By substituting (7) in (4) we find an expression for the output compressed electrical voltage

$$v_o(t) = \frac{1}{2}\kappa L^2\alpha^2 e_0^2 \times \left[S_0\frac{\sin(2\pi\,B\,t)}{\pi\,t} + {\rm dc}_v + V_{\rm bias} - V_\pi\right]^2. \quad (8)$$

Then we find the compressed pulse peak voltage as

$$V_c = \frac{1}{2}\kappa L^2\alpha^2 e_0^2 \left[\sqrt{2UB} + {\rm dc}_v + V_{\rm bias} - V_\pi\right]^2. \quad (9)$$

From (8), the dc level of the output compressed pulse voltage over its temporal window can be approximated. It can be shown that the dc level of the sinc function over the time aperture $\Delta{\rm T}$ can be neglected compared to ${\rm dc_v}$ when the time-bandwidth product $\Delta{\rm TB}$ is large. Then

$${\rm dc}_c = \frac{1}{2}\kappa L^2\alpha^2 e_0^2({\rm dc}_v + V_{\rm bias} - V_\pi)^2 \quad (10)$$

The term ${\rm V_{bias} - V_\pi}$ can be made negligible by biasing the modulator close to its minimum transmission. For an input electrical waveform that spreads extensively enough over time the resulting output uncompressed signal dc voltage over its time window will be much smaller than the output compressed waveform peak voltage, in other words $\sqrt{2\,U\,B} \gg {\rm dc}_v + V_{\rm bias} - V_\pi$. Thus, we can show through (8) that the compressed pulse FWHM duration $\Delta{\rm t}$ is approximately given by $\Delta t \approx 0.44/B$. Defining the maximum peak voltage of ${\rm v_i(t)}$ as ${\rm V_p}$, we write the output uncompressed waveform peak voltage from (5) as

$$V_u = \frac{1}{2}\kappa L^2\alpha^2 e_0^2 \left[V_p + V_{\rm bias} - V_\pi\right]^2. \quad (11)$$

Finally, by substituting in the gain parameter expression, we will obtain

$$\gamma = \frac{2UB + 2\sqrt{2UB}({\rm dc}_v + V_{\rm bias} - V_\pi)}{\left[V_p + V_{\rm bias} - V_\pi\right]^2 - \frac{1}{\Delta T}\int_0^{\Delta T}\left[v_i(\tau) + V_{\rm bias} - V_\pi\right]^2 d\tau.} \quad (12)$$

In order to achieve further intuition in (12), we provide an approximate analytical solution for a simple case. We assume ${\rm v_i(t)}$ as a linear frequency-modulated signal, which is long enough to span many frequency-modulation oscillations, as

$$v_i(t) = \begin{cases} \frac{V_p}{2}\left[\cos\left(\pi\frac{B}{\Delta T}t^2 + \pi\right) + 1\right] & \text{for } 0 \le {\rm t} \le \Delta{\rm T} \\ 0 & \text{elsewhere} \end{cases}. \quad (13)$$

If the signal time-bandwidth product is much larger than 1, or in other words there are many oscillations in the signal temporal

window then by approximating the dc level and the ac energy of the signal, and the associated integrals, we can show

$$\gamma \approx \frac{\frac{2}{5}\Delta T\, B + \frac{4}{5}\sqrt{\Delta T\, B} + \frac{8}{5}\sqrt{\Delta T\, B}\frac{V_{\rm bias}-V_\pi}{V_p}}{1+\frac{8}{5}\frac{V_{\rm bias}-V_\pi}{V_p}}. \qquad (14)$$

This expression shows that the theoretical gain parameter for a linear chirp signal is decreasing by increasing $\mathrm{V_{bias}} - \mathrm{V}_\pi$ and it takes its maximum value for $\mathrm{V_{bias}} = \mathrm{V}_\pi$. For $\mathrm{V_{bias}} = \mathrm{V}_\pi$, which corresponds to a bias point at the minimum transmission of the modulator we define the maximum gain parameter γ_0

$$\gamma_0 = \frac{2}{5}\Delta T\, B + \frac{4}{5}\sqrt{\Delta T\, B}. \qquad (15)$$

By substituting for Δt, we finally obtain

$$\gamma_0 \approx 0.176\eta + 0.531\sqrt{\eta}. \qquad (16)$$

Equations (15) and (16) show that for large values of compression factor, i.e., an input chirp waveform has a large time-bandwidth product, the maximum gain parameter becomes approximately proportional to compression factor with a factor of 0.176. This expression gives us a rough estimate of an achievable gain parameter versus compression factor. The foregoing analyses can also be performed through Fourier series instead of Fourier transform, which again results in (14) for a periodic waveform with temporal window ΔT set equal to the repetition period.

IV. Experimental and Numerical Results

To test our scheme, we have synthesized linear frequency-modulated (chirp) and 15-bits pseudorandom sequence electrical waveforms via the microwave photonic arbitrary waveform generator and used these as inputs to the microwave photonic filter. Due to the roll-off in the frequency responses of the MZM, the pulse shaper, and the photodiode, the output waveform that is obtained from the microwave photonic filter when the pulse shaper is quiescent is not exactly the same as the input waveform to the microwave photonic filter; in fact, the features with higher frequency content are more attenuated. In order to overcome this distortion, we preequalize input waveforms to the microwave photonic filter to obtain a desired waveform at the output when the pulse shaper is quiescent. As an example, for a chirp input waveform, the faster oscillations undergo higher attenuation due to frequency roll-off of the MZM, the pulse shaper, and the photodiode; hence, at the input we synthesize the faster oscillations with larger amplitude in order to achieve a chirp waveform with uniform amplitude at the output. This preequalization does not change the basics of our matched filtering technique and can be eliminated in the future by using components with a uniform frequency response over the desired bandwidth. Hence, we evaluate the performance of our matched filter based on the uncompressed and compressed electrical voltage waveform measured at the output of the microwave photonic filter. First, the uncompressed output waveform that is obtained from the microwave photonic filter when the pulse shaper is quiescent is measured using a fast (50 GHz) sampling scope. Then the spectral phase of the output RF baseband waveform is extracted through fast Fourier transform (FFT). By programming the pulse shaper to apply the opposite spectral phase function, the output electrical waveform is compressed to a short bandwidth-limited electrical pulse.

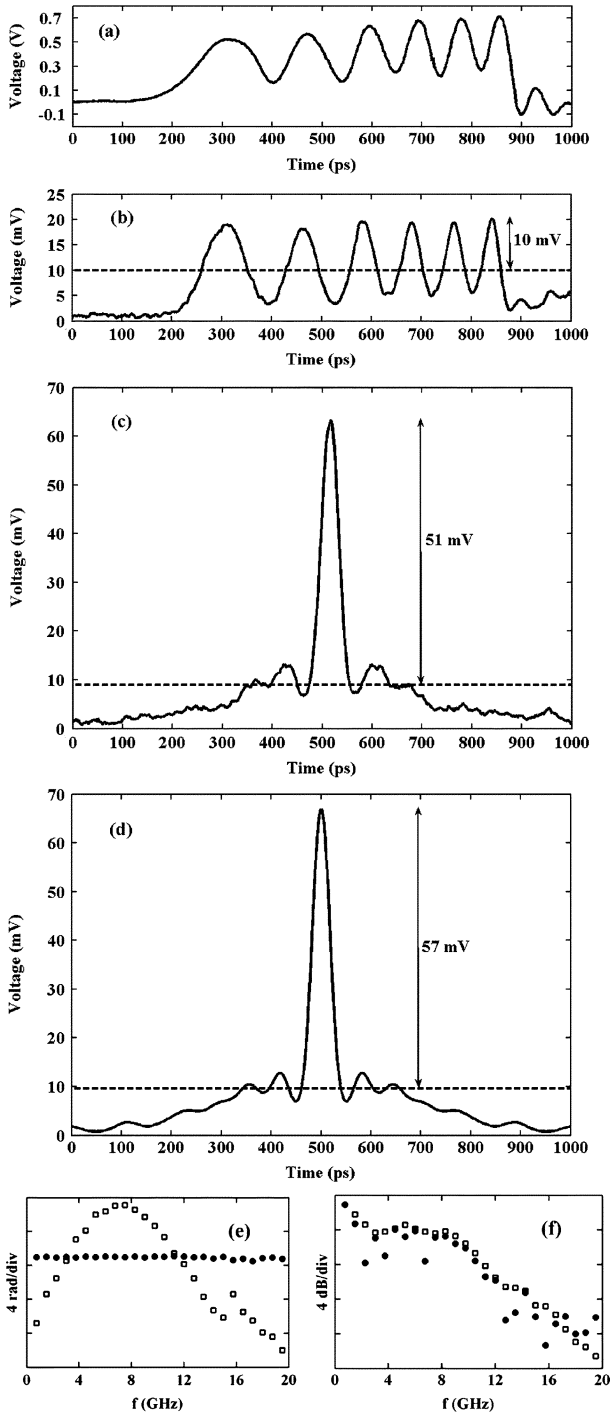

Fig. 5. (a) Experimentally synthesized input linear chirp electrical waveform with $>$ 15 GHz frequency content centered at $\sim$ 7.5 GHz. (b) Experimental output linear chirp electrical waveform when the pulse shaper is quiescent. (c) Experimental output compressed electrical waveform after the matched filter is applied. (d) Calculated ideal photonically matched filtered electrical waveform. (e) Calculated spectral phases of the waveforms in (b) and (c) are shown in squares and bold circles respectively. (f) Calculated spectral amplitudes of the waveforms in (b) and (c) are shown in squares and bold circles, respectively.

Fig. 5 shows matched filtering for a UWB RF electrical chirp waveform. This waveform is designed with a spectrum centered at $\sim$7.5 GHz, an $\sim$ 733 ps temporal window, and the fastest oscillation cycle corresponding to $\sim$ 15 GHz. Fig. 5(a) shows the preequalized UWB RF chirp waveform synthesized via the microwave photonic waveform generator which is applied to the microwave photonic filter. Fig. 5(b) shows the microwave photonic filter output electrical waveform when the pulse shaper is quiescent. As a result of the preequalization, the amplitude of the chirp waveform in Fig. 5(b) is more uniform in time than the input chirp waveform in Fig. 5(a), and the individual oscillations have become sharper due to the squaring operation in (11). The spectral phase and amplitude of the chirp waveform are calculated through FFT and shown by squares in Fig. 5(e) and (f) respectively. The large quadratic spectral phase is consistent with the linearly chirp waveform design. Fig. 5(c) shows the compressed electrical waveform at the output after the conjugate spectral phase, i.e., the matched filter, is applied through the microwave photonic filter. The spectral phase and amplitude of the compressed waveform are shown by bold circles in Fig. 5(e) and (f), which show that the spectral phase is compensated with an error less than 0.2 rad from dc to 15 GHz. A 14.21–dB gain parameter has been achieved, and the output electrical voltage pulse FWHM duration is 40 ps which corresponds to a compression factor of 18.3. A calculation of the electrical waveform of Fig. 5(b) processed through an ideal conjugate spectral phase optical filter which is numerically performed through FFT in MATLAB is shown in Fig. 5(d). For the ideally matched filtered waveform, a 15.11–dB gain parameter and a 38–ps FWHM electrical voltage pulse duration, which corresponds to a compression factor of 19.3, are expected. In each trace the dashed line shows the dc level of the photodiode output voltage waveform averaged over its 733 ps temporal window from 148 to 880 ps. The excellent agreement between experiment and simulation suggests that the uncompressed RF waveform spectral phase is being corrected with a high degree of precision. The slight difference between the uncompressed and compressed spectral amplitudes is expected since the phase programming in SLM introduces some loss which is due to the abrupt phase change between adjacent SLM pixels. To compare the experimental gain with our theoretical analysis we may calculate the gain parameter from (16) which predicts a gain parameter of $5.73 = 15.16$ dB from the experimental compression factor. We may also calculate the maximum theoretical gain parameter through (15) for which we find a gain parameter of $7.05 = 16.96$ dB for the nominal time-bandwidth product. This is in agreement with experiment in which the modulator may not be biased exactly at its minimum transmission.

We have also performed matched filtering for UWB RF electrical chirp waveforms similar to Fig. 5 for different frequency bandwidths. Fig. 6 shows the summary of results. The gain parameters versus frequency bandwidth are plotted for linear frequency-modulated electrical waveforms with fastest oscillation cycles correspond to frequencies of about 7.5, 10, 12.5, and 15 GHz where the temporal aperture is fixed to $\sim$733 ps. The circles illustrate the achieved gain parameter through experiment. The squares show the gain parameter after processing the electrical chirp waveforms through an ideal optical phase-only matched filter in simulation. The dashed line shows the maximum theoretical gain parameter when the bias voltage V_{bias} equals to V_π which is given by (15). The difference between an ideal matched filter gain parameter and a theoretical gain parameter predicted by (15) comes from the simplifying assumptions and approximations that have been made in our derivation. Hence Fig. 6 illustrates the behavior of a matched filter performance which is in excellent agreement with our experimental and numerical results.

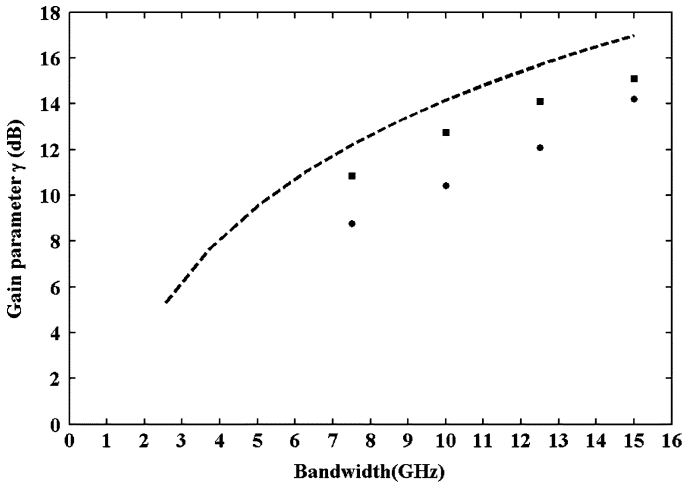

Fig. 6. Gain parameter versus frequency bandwidth for UWB RF chirp electrical waveforms. The circles show the experimental gain parameter versus the frequency corresponding to the chirp fastest oscillation cycle. The squares show the calculated gain parameter after processing waveforms through an ideal photonically matched filter. The dashed line shows the maximum theoretical gain parameter given by (15).

As another example, Fig. 7 shows matched filtering for a 15-chip pseudorandom code (001001101011110) UWB RF electrical waveform at a chip rate corresponding to $\sim$18.7 Gb/s with $\sim$800 ps temporal window. Fig. 7(a) shows the preequalized UWB RF 15-bit pseudorandom waveform synthesized via the microwave photonic waveform generator. Fig. 7(b) shows the microwave photonic filter output electrical waveform when the pulse shaper adds no spectral phase. The spectral phase and amplitude of the pseudorandom waveform are calculated by Fourier transform of the data in Fig. 7(b) and are shown by squares in Fig. 7(e) and (f), respectively. Fig. 7(c) shows the compressed electrical waveform at the photodiode output after the conjugate spectral phase is applied. The spectral amplitude and phase of the compressed waveform are shown by bold circles in Fig. 7(e) and (f), respectively, which show that the spectral phase is compensated with an error less than 0.2 rad from dc to 15.5 GHz. A 14.07–dB gain parameter has been achieved, and the output electrical voltage pulse FWHM duration is 50 ps which corresponds to a compression factor of 16. A calculation of the electrical waveform of Fig. 7(b) processed through an ideal conjugate spectral phase optical filter is shown in Fig. 7(d). For the ideally matched filtered electrical waveform, a 14.85–dB gain parameter and a 46–ps FWHM pulse duration, which corresponds to a compression factor of 17.4, are expected. Here also the excellent agreement between experiment and simulation suggests that the uncompressed RF

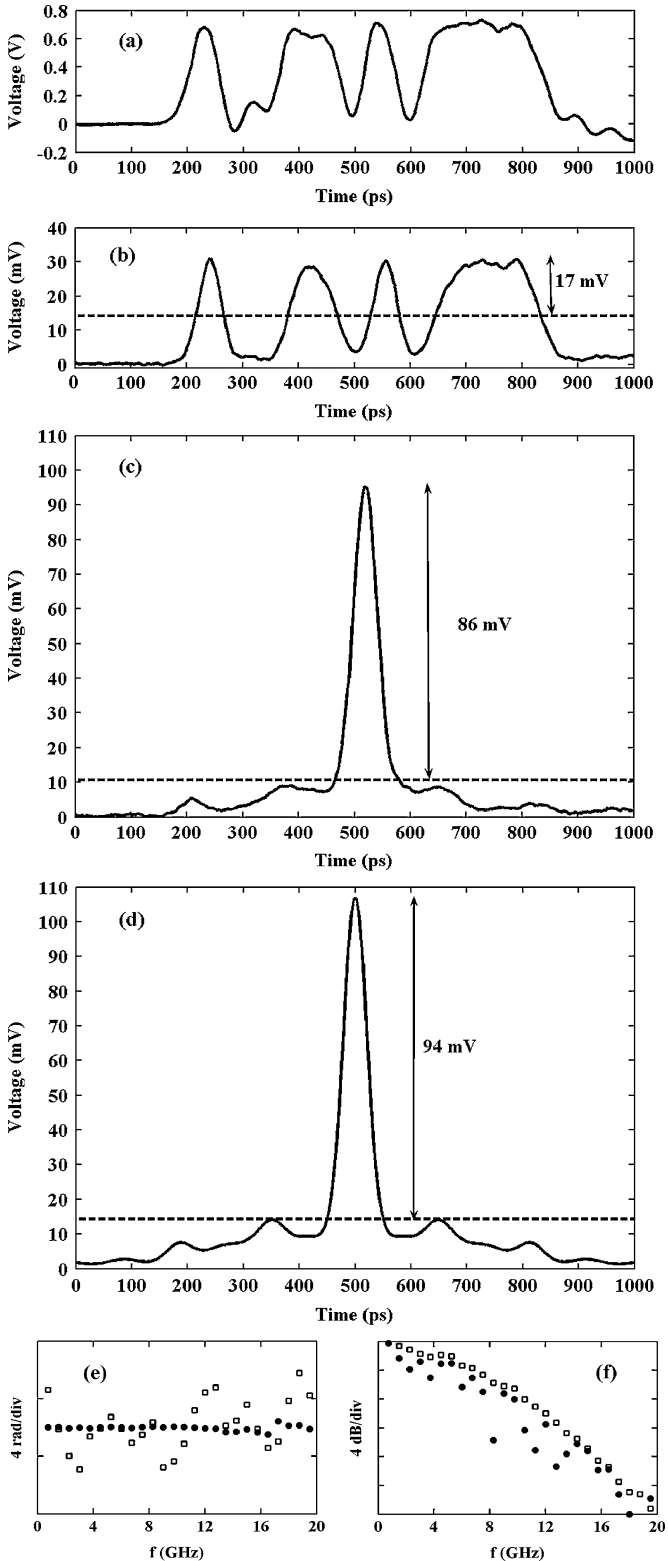

Fig. 7. (a) Experimentally synthesized input 15-chip pseudorandom electrical waveform. (b) Experimental output 15-chip pseudorandom electrical waveform when the pulse shaper is quiescent. (c) Experimental output compressed electrical waveform after the matched filter is applied. (d) Calculated ideal photonically matched filtered electrical waveform. (e) Calculated spectral phases of the waveforms in (b) and (c) are shown in squares and bold circles, respectively. (f) Calculated spectral amplitudes of the waveforms in (b) and (c) are shown in squares and bold circles, respectively.

electrical waveform is matched filtered with a high degree of precision.

The matched filtering technique can be applied to compress and asynchronously detect spread-time waveforms which are arbitrarily spectral encoded. This includes a wide range of waveforms; however, waveforms such that their spectrum almost uniformly covers a baseband spectrum, e.g., a linear frequency-modulated waveform, have been our focus here. This group of waveforms carries the maximum energy for a given bandwidth and maximum allowed power spectrum level that enables their power spectrum to be buried in a background noise. This property makes them good candidates for UWB applications, multiple access systems, and low probability of intercept systems in secure communication. This group may be categorized as spectral phase-only encoded waveforms. It can be shown that the maximum gain parameter and the maximum compression factor can be achieved by matched filtering these waveforms for a given bandwidth and a temporal window.

Currently, our microwave photonic filter has an RF transmission coefficient, from the MZM input electrical voltage to the photodiode output electrical voltage, of about -30 dB. Taking into account the compression gain of the waveforms reported above, this figure would become as high as -16 dB. This already surpasses the overall RF gain (including compression gain) of -23 dB for the 1.1–GHz bandwidth SAW filter reported in [24]. The RF gain in our system can be enhanced by using a higher power CW laser source, a MZM with lower insertion loss and with lower V_π (commercially available down to 1 V), and a photodiode with higher responsivity and power handling capability. On the other hand, the hyperfine resolution pulse shaper has an insertion loss of ~ 14 dB which theoretically may be reduced down to ~ 8 dB that will further improve the transmission coefficient [30]. The nonlinearity due to the MZ intensity modulator can be mitigated by direct modulation of distributed feedback laser (DFB), which has a more linear transfer characteristic compared to $LiNbO_3$ MZM [31].

V. Conclusion

We experimentally demonstrate compression of UWB RF spread-time arbitrary electrical waveforms via programmable microwave photonic phase filters implemented in an optical pulse shaper. This opens a new approach to compress and asynchronously detect RF electrical waveforms in UWB communication systems via matched filtering. This enables to asynchronously detect UWB spread-time electrical waveforms, to recover a synchronizing signal, and to compensate a channel response due to antenna dispersion at a receiver front. This technique is also a possible solution for multicode UWB system using chirp waveforms [32], UWB high resolution ranging system [33], and UWB radar with millimeter resolution [34].

Acknowledgment

The authors would like to thank our colleague I. S. Lin for helping with the microwave photonic arbitrary waveform generation setup, our lab manager D. E. Leaird for his helpful technical assistance and discussion on this project, and C. Lin, Avanex Corporation, Fremont, CA, for providing VIPA devices.

REFERENCES

[1] K. Wilner and A. P. Van Den Heuvel, "Fiber-optic delay lines for Microwave signal processing," *Proc. IEEE*, vol. 64, no. 5, pp. 805–807, May 1976.

[2] Y. Liu, J. Yang, and J. Yao, "Continuous true-time-delay beam forming for phased array antenna using a tunable chirped fiber grating delay line," *IEEE Photon. Technol. Lett.*, vol. 14, no. 8, pp. 1172–1174, Aug. 2002.

[3] A. Seeds, "Microwave photonics," *IEEE Trans. Microw. Theory Tech.*, vol. 50, no. 3, pp. 877–887, Mar. 2002.

[4] R. A. Minasian, "Photonic signal processing of microwave signals," *IEEE Trans. Microw. Theory Tech.*, vol. 54, no. 2, pp. 832–846, Feb. 2006.

[5] J. Capmany, B. Ortega, and D. Pastor, "A tutorial on microwave photonic filters," *J. Lightw. Technol.*, vol. 24, no. 1, pp. 201–229, Jan. 2006.

[6] J. Capmany, B. Ortega, D. Pastor, S. Sales, P. Y. Fonjallaz, M. Popoy, L. Pierno, and M. Varasi, "Microwave photonic signal processing for wireless systems and optical Internet: Overview of the current achievements of the IST-LABELS project," in *Proc. 6th Int. Conf. Transparent Opt. Netw.*, 2004, vol. 2, pp. 8–12.

[7] S. Xiao and A. M. Weiner, "Programmable photonic microwave filters with arbitrary ultra-wideband phase response," *IEEE Trans. Microw. Theory Tech.*, vol. 54, no. 11, pp. 4002–4008, Nov. 2006.

[8] S. Xiao and A. M. Weiner, "Coherent photonic processing of microwave signals using spatial light modulator: Programmable amplitude filters," *J. Lightw. Technol.*, vol. 24, no. 7, pp. 2523–2529, Jul. 2006.

[9] J. Chou, Y. Han, and B. Jalali, "Adaptive RF-photonic arbitrary waveform generator," *IEEE Photon. Technol. Lett.*, vol. 15, no. 4, pp. 581–583, Apr. 2003.

[10] J. D. McKinney, D. S. Seo, D. E. Leaird, and A. M. Weiner, "Photonically assisted generation of arbitrary millimeter-wave and microwave electromagnetic waveforms via direct space-to-time optical pulse shaping," *J. Lightw. Technol.*, vol. 21, no. 12, pp. 3020–3028, Dec. 2003.

[11] I. S. Lin, J. D. McKinney, and A. M. Weiner, "Photonic synthesis of broadband microwave arbitrary waveforms applicable to ultra-wideband communication," *IEEE Microw. Wireless Compon. Lett.*, vol. 15, no. 4, pp. 226–228, Apr. 2005.

[12] T. Yilmaz, C. M. DePriest, T. Turpin, J. H. Abeles, and P. J. Delfyett, "Toward a photonic arbitrary waveform generator using a modelocked external cavity semiconductor laser," *IEEE Photon. Technol. Lett.*, vol. 14, no. 11, pp. 1608–1610, Nov. 2002.

[13] Q. Wang and J. Yao, "Switchable optical UWB monocycle and doublet generation using a reconfigurable photonic microwave delay-line filter," *Opt. Express*, vol. 15, no. 22, pp. 14667–14672, Oct. 2007.

[14] G. L. Turin, "An introduction to matched filters," *IRE Trans. Inf. Theory*, vol. IT-6, no. 3, pp. 311–329, Jun. 1960.

[15] J. G. Proakis, *Digital Communications*, 4th ed. New York: McGraw-Hill, 2001.

[16] R. A. Scholtz, D. M. Pozar, and W. Namgoong, "Ultra-wideband radio," *EURASIP J. Appl. Signal Process.*, vol. 3, pp. 252–272, Mar. 2005.

[17] W. M. Lovelace and J. K. Townsend, "The effects of timing jitter and tracking on the performance of impulse radio," *IEEE J. Sel. Areas Commun.*, vol. 20, pp. 1646–1651, Dec. 2002.

[18] I. S. Lin and A. M. Weiner, "Selective correlation detection of photonically generated ultrawideband RF signals," *J. Lightw. Technol.*, vol. 26, no. 15, pp. 2692–2699, Aug. 1, 2008.

[19] P. Tortoli, F. Guidi, and C. Atzeni, "Digital vs SAW matched filter implementation for radar pulse compression," in *Proc. IEEE Ultrason. Symp.*, 1994, vol. 1, pp. 199–202.

[20] J. A. Salehi, A. M. Weiner, and J. P. Heritage, "Coherent ultrashort light pulse code-division multiple access communication systems," *J. Lightw. Technol.*, vol. 8, no. 3, pp. 478–491, Mar. 1990.

[21] P. M. Crespo, M. L. Honig, and J. A. Salehi, "Spread-time code-division multiple access," *IEEE Trans. Commun.*, vol. 43, no. 6, pp. 2139–2148, Jun. 1995.

[22] J. H. Reed, *An Introduction to Ultra Wideband Communication Systems*. Upper Saddle River, NJ: Prentice-Hall, 2005.

[23] A. M. Weiner, "Femtosecond pulse shaping using spatial light modulators," *Rev. Sci. Instrum.*, vol. 71, no. 5, pp. 1929–1960, May 2000.

[24] R. Brocato, J. Skinner, G. Wouters, J. Wendt, E. Heller, and J. Blaich, "Ultra-wideband SAW correlator," *IEEE Trans. Ultrason., Ferroelectr., Freq. Control*, vol. 53, no. 9, pp. 1554–1556, Sep. 2006.

[25] First Report and Order (Revision of Part 15 of the Comission's Rules Regarding Ultra-Wideband Transmission Systems) Washington, DC, FCC eT Docket, adopted, released April 22, 2002, Feb. 14, 2002, pp. 98–153.

[26] I. H. Wang and S. I. Liu, "A 1 V 5-Bit 5 GSample/sec CMOS ADC for UWB receivers," in *Proc. Tech. Papers 2007 Int. Symp. VLSI Design, Automa. Test*, Apr. 2007, pp. 140–143.

[27] J. Han, R. Xu, and C. Nguyen, "Development of a low-cost, compact planar synchronous receiver for UWB systems," in *IEEE Antennas Propag. Soc. Int. Symp.*, Jul. 2006, pp. 1287–1290.

[28] M. Shirasaki, "Large angular dispersion by a virtually imaged phased array and its application to a wavelength demultiplexer," *Opt. Lett.*, vol. 21, no. 5, pp. 366–368, Mar. 1996.

[29] W. S. C. Chang, *RF Photonic Technology in Optical Fiber Links*, 1st ed. Cambridge, U.K.: Cambridge Univ. Press, 2002, pp. 84–90.

[30] M. Shirasaki, "Chromatic-dispersion compensator using virtually imaged phased array," *IEEE Photon. Technol. Lett.*, vol. 9, no. 12, pp. 1598–1600, Dec. 1997.

[31] H. Yonetani, I. Ushijima, T. Takada, and K. Shima, "Transmission characteristics of DFB laser modules for analog applications," *J. Lightw. Technol.*, vol. 11, no. 1, pp. 147–153, Jan. 1993.

[32] H. Liu, "Multicode ultra-wideband scheme using chirp waveforms," *IEEE J. Sel. Areas Commun.*, vol. 24, no. 4, pp. 885–891, Apr. 2006.

[33] J. Y. Lee and R. A. Scholtz, "Ranging in a dense multipath environment using an UWB radio link," *IEEE J. Sel. Areas Commun.*, vol. 20, no. 9, pp. 1677–1683, Dec. 2002.

[34] J. Dederer, B. Schleicher, F. De Andrade Tabarani Santos, A. Trasser, and H. Schumacher, "FCC compliant 3.1–10.6 GHz UWB pulse radar system using correlation detection," in *Proc. IEEE MTT-S Int. Microw. Symp. Dig. 2007*, 2007, pp. 1471–1474.

Ehsan Hamidi (S'08) was born in Tehran, Iran, in 1983. He received the B.S. degree in electrical engineering from Sharif University of Technology, Tehran, in 2005.

He is currently working toward the Ph.D. degree at Purdue University, West Lafayette, IN. He has been a Research Assistant with the School of Electrical and Computer Engineering since 2005. His current research interests include microwave photonics with applications in ultrawideband communication, ultrafast optics, optical pulse shaping, and optical fiber communications.

Mr. Hamidi is a Student Member of the IEEE Lasers and Electro-Optics Society and the IEEE Communication Society. He has served as a reviewer for the JOURNAL OF LIGHTWAVE TECHNOLOGY.

Andrew M. Weiner (S'84-M'84-SM'91-F'95) received the Sc.D. degree in electrical engineering from the Massachusetts Institute of Technology (MIT), Cambridge, in 1984.

From 1979 to 1984, he was a Fannie and John Hertz Foundation Graduate Fellow with MIT. Upon graduation, he joined Bellcore, first as Member of Technical Staff and later as Manager of Ultrafast Optics and Optical Signal Processing Research. He moved to Purdue University, West Lafayette, IN, in 1992 and is currently the Scifres Distinguished Professor of Electrical and Computer Engineering. His research focuses on ultrafast optics signal processing and applications to high-speed optical communications and ultrawideband wireless. He is especially well known for his pioneering work in the field of femtosecond pulse shaping. He has published six book chapters and more than 200 journal articles. He has been the author or coauthor of more than 350 conference papers, including approximately 80 conference invited talks, and has presented nearly 100 additional invited seminars at university, industry, and government organizations. He holds 10 U.S. patents.

Prof. Weiner is a Fellow of the Optical Society of America and is a Member of the U.S. National Academy of Engineering. He was the recipient of numerous awards for his research, including the Hertz Foundation Doctoral Thesis Prize (1984), the Adolph Lomb Medal of the Optical Society of America (1990), awarded for pioneering contributions to the field of optics made before age 30, the Curtis McGraw Research Award of the American Society of Engineering Education (1997), the International Commission on Optics Prize (1997), the IEEE LEOS William Streifer Scientific Achievement Award (1999), the Alexander von Humboldt Foundation Research Award for Senior U.S. Scientists (2000), and the OSA R.W. Wood Prize (2008). He has been recognized by Purdue University with the inaugural Research Excellence Award from the Schools of Engineering (2003) and with the Provost's Outstanding Graduate Student Mentor Award (2008).